

## Fabrication and Characterization of ZnS<sub>Cubic</sub> : P3HT, ZnS<sub>Hexa</sub> : P3HT and ZnS<sub>Hexa</sub> : P3HT:PVA-Ag Bulk Heterojunction Solar Cells

T. Abdul Kareem<sup>1,\*</sup>, A. Anu Kaliani<sup>2</sup>

<sup>1</sup> Department of Physics, University of Calicut, 673635 Kerala, India

<sup>2</sup> Department of Physics, Kongunadu Arts and Science College, 641029 Coimbatore, Tamilnadu, India

(Received 02 April 2015; published online 10 June 2015)

This paper describes the fabrication of P3HT based bulk heterojunction solar cell using ZnS nanoparticles of sphalerite and wurtzite crystal structure and discusses their photovoltaic characteristics. It is found that the device of P3HT : ZnS can give higher  $V_{oc}$  and surface modified wurtzite ZnS is able to give higher  $V_{oc}$  ( $\sim 1.3$  V) as well as higher current density ( $229.60 \mu\text{A}/\text{cm}^2$ ) and comparable efficiency (0.032 %). Active layer (P3HT : ZnS) showed a broad optical absorption from 320 nm to 650 nm and it is seen that the absorption intensity increased in the blend than the pristine P3HT.

**Keywords:** ZnS nanoparticles, Solar cells, High  $V_{oc}$ .

PACS numbers: 78.20. – e, 78.40.Fy, 78.56. – a,  
78.67. – n, 88.40.jr

### 1. INTRODUCTION

Bulk heterojunction solar cells made of conducting polymers represent a new phase in the evolution of photovoltaic devices and these types of excitonic cells are presently the most studied solar cells. In the case of bulk heterojunction, electron accepting nanoparticles are mixed with the electron donating polymer and the exciton created in the polymer material diffuse to the donor-accepter interface to enable the charge separation. There are three main reasons for preferring bulk heterojunction than multilayer or heterojunction polymer solar cells, one of them is the binding energy of the polymeric excitons, which is in the range of 0.2 eV-0.4 eV [1, 2] and that is considerably higher than the binding energy for inorganic semiconductor materials. Second is the life time of the exciton in the conjugated polymer which is about sub-nanoseconds [1] and the third is the small diffusion range which is about 5 nm-10 nm [2]. For efficient charge generation after absorption of light, each exciton has to find a donor – acceptor interface within femtoseconds within few nano meter, otherwise it will be lost without charge generation. These properties results in a poor efficiency of the heterojunction or multilayer organic photovoltaic devices and that can be solved by incorporating semiconducting nanoparticles into the polymer matrices since polymer materials phase separate on a nanometer dimension. This mixing of the  $p$  and  $n$  type materials create junctions throughout the bulk of the material that ensure quantitative dissociation of photo generated excitons irrespective of the thickness. In such hybrid (organic and inorganic) materials, organic polymer acts as electron donor and the inorganic nanoparticles as an electron acceptor. So that the positive charges move by hole hopping, and the negative charges by electron hopping via charge transfer between molecules. The advantage of hybrid bulk heterojunction cells is that both the organic and inorganic materials contribute to the photocurrent [3].

Various combinations of donor and acceptor materials have been used to build bulk heterojunction solar cells in which the composite active layer is inserted between two electrodes. Polymer – fullerene (polymer-PCBM) solar cells are most studied combination bulk heterojunction cells [3-5]. The holes are transported by the  $p$  type polymeric semiconductor and the electrons by the  $n$  type nano materials and both these materials should be preferably mixed into a bicontinuous interpenetrating network. As a result of the intimate mixing, the interface where charge transfer can occur has increased enormously. The exciton created after the absorption of light has to diffuse towards this charge transfer interface for charge generation to occur.

There are about 3500 research papers including patents until this date discussing the P3HT : PCBM BHJ solar cells in google scholar, where P3HT acts as a photon absorber and a donor and fullerene derivatives PCBM acts as an acceptor. However, there are some limitations in the P3HT / PCBM blend solar cells that low charge mobility, weak absorption in the visible spectrum, and low open circuit voltage ( $V_{oc}$ ) (about 0.6 V [6]) due to the extremely deep lying lowest unoccupied molecular orbital (LUMO) levels of PCBM. Researchers are working with a lot of different types of organic (polymer) solar cells. Among them, the organic-inorganic hybrid solar cell is promising because of the advantages resulting from two types of materials with low cost and easy preparation from organic material, high electron mobility, and excellent chemical and physical stability. In order to find electron accepting and hole conducting materials with a better match, one needs to know the energy of their levels involved in the photovoltaic process. Since, the open circuit voltage ( $V_{oc}$ ) of bulk heterojunction solar cells is governed by the HOMO of the donor and the LUMO levels of the acceptor and at least 0.3 eV difference is needed in between the LUMOs of the donor and acceptor for exciton dissociation and a forward electron transfer from the donor to the acceptor ( $E_{\text{LUMO (Acceptor)}} - E_{\text{LUMO (Donor)}} > \text{Exciton binding energy}$ ).

\* [abdulkareem.t@gmail.com](mailto:abdulkareem.t@gmail.com)

This paper discusses the use of inorganic semi conducting ZnS nanoparticles with P3HT and it is preferred as an electron acceptor because it is environment friendly, stable indefinitely, and can be synthesized easily and inexpensively. It is supposed that the LUMO level of the inorganic semiconductor is below at least 0.3 eV than that of P3HT for an effective exciton splitting and charge dissociation [7], since quantum confinement effect of the semiconducting nanocrystals shifts their LUMO level to upward and the HOMO to downward and that enlarges the band gap [8]. The wide band semiconductor ZnS has high electron mobility ( $600 \text{ cm}^2\text{V}^{-1}\text{s}^{-1}$  [9]) and has an electron affinity of about 3.9 eV [10] that makes ZnS as an attractive material to use as an electron acceptor in hybrid photovoltaic devices. Further, conduction band shifts upward as decreasing the size of the particle [8] that helps to match well with the LUMO level of P3HT, therefore ZnS nanoparticles provide the right morphology for the acceptance of electron.

Previously Bredol et al. [11] showed that a high  $V_{oc}$  ( $\sim 1.2 \text{ V}$ ) can be achieved in a system prepared from P3HT in contact with ZnS nanoparticles (where the ZnS content is 50 wt %,  $I_{sc}$  is  $0.0081 \text{ mA/cm}^2$ , 0.2 % efficiency, and FF is 25 %). However, the efficiency is rather low (0.2 %), partly due to the negligible contribution from ZnS to the photocurrent but in the case of P3HT : ZnS cell prepared by Mall et al. [12], ZnS quantum dots offered better pathways to electrons that reduced the series resistance. Further the cell performance can be improved by modifying the surface of the ZnS particles and the absorption of hybrid solar cells can also be increased by the trapping the light inside the active layer using metal nano particles. These types of solar cells are known as plasmonic solar cells [13]. The new design utilizes the surface plasmon resonance (SPR) excitation and generally there are three ways of enhancing the optical absorption in solar cells: metallic nanoparticles or periodic structures integrated on top of the absorbing material [14], metallic nanoparticles integrated into the active materials [15], and metallic periodic structures and random metallic nanoparticles placed on the backcontact surface [16, 17]. Although the introduction of metal nano particles enhances absorption, it also alters the operation of organic solar cells in ways that are detrimental to device performance. The excitation of LSPR through the resonant interaction between the electromagnetic field of incident light and the surface electron density surrounding metallic nanoparticles causes local enhancement in the electromagnetic field, which is expected to enhance light harvesting in the OPV devices. This paper also discusses a simple method of doping PVA coated Ag nano particles into the P3HT:ZnS layer to improve the device performance, since metal nano particles strongly scatter lights at wavelength near to their plasmon resonance due to the collective oscillation of the conduction electrons in the metal.

## 2. MATERIALS AND METHODS

Since the performance of bulk heterojunction solar cells strongly depends on the various processing conditions such as film thickness, donor / acceptor mixing

ratio, and thermal annealing time and temperature, all devices for this study were fabricated by considering the previously reported optimized condition for the standard P3HT / PCBM and P3HT / ZnS devices [11].

All chemicals such as PEDOT : PSS, P3HT and indium tin oxide glass slides (surface resistivity is about  $8 \text{ to } 12 \text{ } \Omega/\text{m}^2$  and having thickness about  $1200 \text{ \AA}$ ) were purchased from Sigma Aldrich chemicals Ltd., Bangalore. Sphalerite and Wurtzite ZnS nanoparticles and poly vinyl alcohol coated silver nanoparticles [18] of better performance for the solar cells were prepared in our lab by simple wet chemical method. Here the active layer of the solar cell was sandwiched in between ITO (work function  $\sim 4.8 \text{ eV}$  [19]) and Aluminium (work function  $\sim 4.1 \text{ eV}$  [20]) to generate a built-in electric field caused by the difference in their work functions. This built-in electric field is used to dissociate the excitons generated by the absorption of light in the active layer, where the transparent ITO layer is used as a top electrode facing the sun light. It is a well-known fact that thin film of ITO has low electrical resistivity ( $\sim 5 \times 10^{-4} \text{ } \Omega \text{ cm}$  [21]) and has band gap of about 3.8 eV [22]. Furthermore, ITO is a good hole injector [23] and therefore it can be used as anode. In principle, ITO is capable of collecting either electrons or holes since its work function (ca. 4.2-5.3 eV [1]) lies between the typical HOMO and LUMO of common organic photovoltaic (OPV) materials. Accordingly, the polarity of ITO can be modified to efficiently collect either electrons or holes by coating with functional interlayers of different work functions such as PEDOT : PSS [24], so that 50 nm thick PEDOT : PSS film were coated over the ITO. Solution of PEDOT : PSS was made by mixing PEDOT : PSS (2 ml) and surfactant Triton-100 (50 microliter). Then one drop of the filtered (by a 0.45 micron nylon filter) PEDOT : PSS solution was applied over the ITO to coat the PEDOT : PSS layer at 3000 rpm for 10 seconds to make a film of about 50 nm thick.

Four different samples of P3HT (20 mg/ml in dichlorobenzene) were prepared for comparing device properties. The samples were 1) Pristine P3HT, 2) P3HT mixed with 1 mg of  $\text{ZnS}_{\text{cubic}}$  nano particles 3) P3HT mixed with 1 mg of  $\text{ZnS}_{\text{Hexa}}$  nano particles and the 4<sup>th</sup> sample (P3HT mixed with 1mg of  $\text{ZnS}_{\text{Hexa}}$  nano particles and 1 mg PVA-Ag) was made after studying the solar cell characteristics of the devices made with above 2<sup>nd</sup> and 3<sup>rd</sup> samples. All the samples were kept under stirring for 24 hour, then each drop of the samples were placed over the previously prepared ITO:PEDOT:PSS films and over cleaned plane glass slides also, where the spinner spinned at 3000 rpm for 10 seconds in each case. Where one edge of the plane glass slides was covered with cellophane tape to make 'step' for thickness measurement and the thickness of the active layer found as given in the Table 1 using a noncontact 3D Profiler (Taylor Hobson Talysurf CCI MP interferometer).

A chromium mask with device areas  $1 \times 10^{-6}\text{m}^2$  ( $1 \text{ mm} \times 1 \text{ mm}$ ) and  $4 \times 10^{-6}\text{m}^2$  ( $2 \text{ mm} \times 2 \text{ mm}$ ) was placed over the active layer and kept the samples in the thermal evaporator 10 inch away from the molybdenum boat containing 81 mg of Al pellets. Pressure inside the chamber was maintained as  $5 \times 10^{-5} \text{ mb}$  and applied a voltage of 3 V and 25 A current for coating the Al.

**Table 1** – Thickness of the prepared thin films

Sample Name	Thickness (nm)
Glass / P3HT	15.2
Glass / P3HT : ZnS <sub>Cubic</sub>	247
Glass / P3HT : ZnS <sub>Hexa</sub>	275
Glass / P3HT : ZnS <sub>Hexa</sub> :Ag-PVA	102

Thickness was monitored using the crystal thickness monitor and the coating process was stopped when the thickness was about 105 nm. Final devices are shown in the figure 1, figure 2 and figure 3, where the small devices have area about  $1 \times 10^{-6} \text{ m}^2$  and the bigger is about  $4 \times 10^{-6} \text{ m}^2$ .

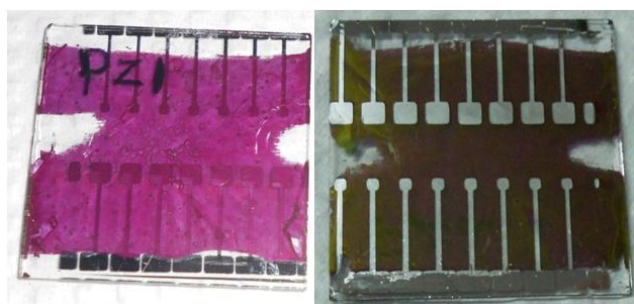


**Fig. 1** – Solar cell of structure ITO / PEDOT : PSS / P3HT : ZnS<sub>Cubic</sub> / Al

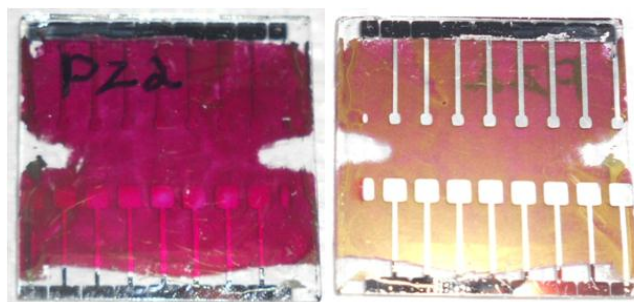


**Fig. 2** – Solar cell of structure ITO / PEDOT : PSS / P3HT : ZnS<sub>Hexa</sub> / Al

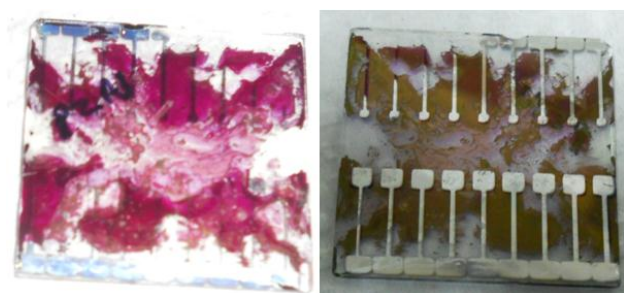


**Fig. 3** – Solar cell of structure ITO / PEDOT : PSS / P3HT : ZnS<sub>Hexa</sub>-PVA@Ag / Al

### 3. RESULTS AND DISCUSSION

Sphalerite and wurtzite ZnS nanoparticles were prepared in our lab using trisodium citrate and polyvinyl alcohol. Their band gap and crystallite sizes are shown in the Table 2, but their preparation methods and other results are not included in this paper since that does not come under the scope of this paper.

From these results the size dependence of conduc-

tion band ( $E_{cb}$ ) and valance band ( $E_{vb}$ ) energies of the prepared nanoparticles can be approximated by

$$E_{cb} = E_{(cb,bulk)} + (E_{(g,observed)} - E_{(g,bulk)})((m_h^*) / (m_h^* + m_e^*)),$$

$$E_{vb} = E_{cb} - E_{(g,observed)},$$

where  $E_{cb}$  and  $E_{cb,bulk}$  ( $-3.9 \text{ eV}$  [10]) are the conduction band energy of the nano particle and bulk respectively, while  $E_{g,observed}$  and  $E_{vb}$  corresponds to the observed band gap and valance band energy of nano crystal,  $m_h^*$  and  $m_e^*$  are effective masses of holes ( $0.6 m_e$  [25]) and electrons ( $0.3 m_e$  [25]). Calculated value of  $E_{cb}$  and  $E_{vb}$  for the synthesized ZnS nano particles are  $-3.43 \text{ eV}$  and  $-7.81 \text{ eV}$  respectively for cubic ZnS and  $-3.79 \text{ eV}$  and  $-7.86 \text{ eV}$  respectively for hexagonal ZnS.  $V_{oc}$  obtained from the polymer P3HT can be calculated from its band gap energy minus  $0.4 \text{ eV}$  for dissociation of the exciton, minus two times  $0.1 \text{ eV}$  for barrier to the electrodes and the expected  $V_{oc}$  is about  $1.3 \text{ eV}$  (i.e.  $1.9 \text{ eV} - 0.4 \text{ eV} - 2 \times 0.1 \text{ eV}$ ). Further the expected  $V_{oc}$  of the P3HT : ZnS system can be calculated from the difference in energy of HOMO of P3HT and LUMO of ZnS as  $1.67 \text{ V}$  in P3HT : ZnS<sub>Cubic</sub> and  $1.31 \text{ V}$  in P3HT : ZnS<sub>Hexa</sub>. A schematic energy level diagram of the P3HT : ZnS blend is given in the figure 4. It is clear from the energy level diagram that the difference of electron affinities of P3HT and ZnS nanoparticles is  $\sim 0.43 \text{ eV}$  for cubic ZnS and  $\sim 0.79 \text{ eV}$  for Hexagonal ZnS, which is larger than the binding energy of the excitons ( $0.4 \text{ eV}$ ) and therefore the charge transfer process is evident in this case.

**Table 2** – Band gap and crystallite sizes of prepared ZnS

ZnS	Crystallite size, nm	Band gap from Brus equation [ ], eV	Band gap from absorption spectra, eV
Sphalerite (Cubic)	1.46	6.82	4.38
Wurtzite (Hexagonal)	3.2	4.45	4.07

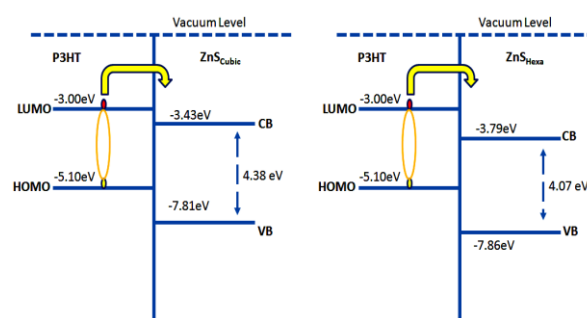


**Fig. 4** – Energy level diagram

UV-Vis measurements of the active layer obtained by Varian, Cary 5000 Spectrophotometer and that can show the absorption and transmission characteristics of the active layer of the solar cells to visible light. Figure 5 shows the absorption spectra of the P3HT : ZnS and P3HT : ZnS : PVA-Ag samples and it shows a broad absorption from  $400 \text{ nm}$  to  $650 \text{ nm}$ . Previous reports of P3HT shows a broad absorption spectra from  $320$  to  $650 \text{ nm}$  and it varied depending on the sol-

vent but around 500 nm, that can be attributed to the  $\pi$ - $\pi^*$  transitions [12]. UV-Vis spectrum of blend shown in the figure 5 is simply the combination of constituents parts of the active materials i.e. nanocrystals and polymer without any additional absorption peaks [12] since there is not any ground state interactions between them [26]. It is seen that the absorption edge of the ZnS : P3HT little extended to the lower wavelength region and that may be due to the quantum confinement effect from the inorganic nano particles [12]. This blue shift may be due to the rising in band gap between  $\pi$  and  $\pi^*$  energy levels when adding the nanoparticles that decreases the inter-chain interaction and conjugation length of P3HT [12]. Remarkable finding here is that the addition of the ZnS in to the P3HT matrix increased the magnitude of the absorption which can be attributed to the crystallization of the P3HT and is thus able to capture more incoming light [27, 28].

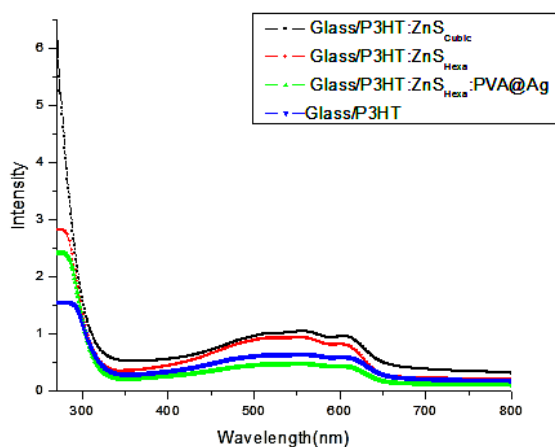


Fig. 5 – Optical absorption spectra of the active materials

Two probe  $I$ - $V$  measurements of the prepared solar cells were noted by Oriel Sol3A. Solar Simulator under illuminated and non illuminated conditions, the results were then compared to determine the improvements in the P3HT based polymer bulk heterojunction solar cells. It is obvious that the absorption in the photoactive blend cannot be 100 % in a real device, because the active layer is embedded within a stack of several layers, which have different complex refractive indexes. For an efficient charge generation in the donor – acceptor blend, a certain offset of the HOMO and LUMO level is required, which is about few milli electron volts. This offset is known as exciton binding energy that determines the ultimate device efficiency of the bulk heterojunction and at least an offset of 0.3 eV is needed for efficient charge generation [3].

$J$ - $V$  characteristics of the fabricated devices are shown in figure 6, figure 7 and in figure 8 and the solar cell parameters are tabled in the Table 3, Table 4 and in Table 5. When comparing the devices with cubic ZnS and hexagonal ZnS, it is seen that the device made of hexagonal ZnS has higher efficiency (0.032) and has higher  $V_{oc}$  (1.3 V). This device shows higher  $J_{sc}$  and  $V_{oc}$  than previously published P3HT : ZnS based systems, that may be due to the surface modification of the ZnS nanoparticles by tri-sodium citrate and polyvinyl alcohol and may be the hexagonal structure.

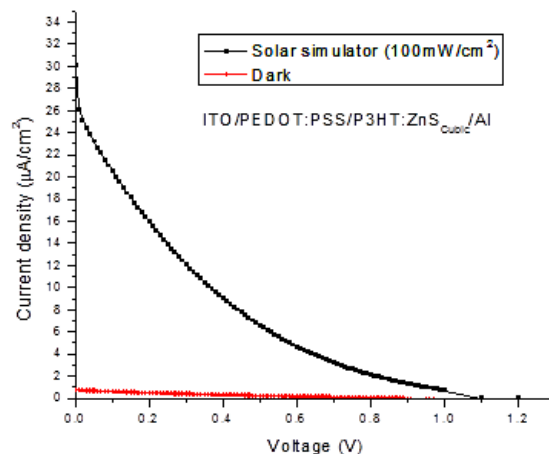


Fig. 6 – Illuminated and non-illuminated  $J$ - $V$  characteristics of ITO / PEDOT : PSS / P3HT : ZnS<sub>cubic</sub> / Al

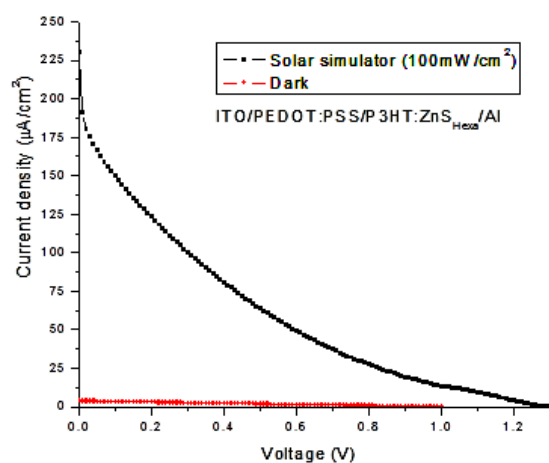


Fig. 7 – Illuminated and nonilluminated  $J$ - $V$  characteristics of ITO / PEDOT : PSS / P3HT : ZnS<sub>Hexa</sub> / Al

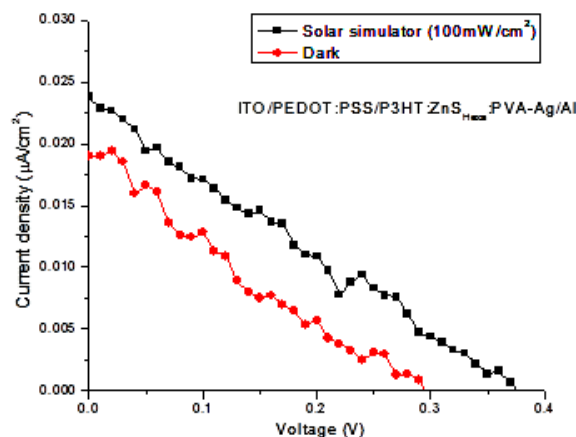


Fig. 8 – Illuminated and nonilluminated  $J$ - $V$  characteristics of ITO / PEDOT : PSS / P3HT : ZnS<sub>Hexa</sub> : PVA-Ag / Al

The third device was made with mixing the Polyvinyl alcohol coated silver nanoparticles with the improved cell structure hexagonal ZnS. Since, metallic nanoparticles are well known for their strong interactions with visible light, which arise because of the localized surface plasmon resonances (LSPR) of the collective oscillations of the conduction electrons within the

**Table 3** – Solar cell parameters of the device ITO / PEDOT : PSS / P3HT : ZnS<sub>CUBIC</sub> / Al

Mode	$P_{max}$ , nW	$I_{pm}$ , nA	$V_{pm}$ , V	$J_{sc}$ , $\mu\text{A}/\text{cm}^2$	$V_{oc}$ , V	$FF$	$E_{ff}$ , %	$R_s$ , M $\Omega$	$R_{sh}$ , M $\Omega$
Light	146.441	430.708	0.340	30.100	1.120	0.109	0.0037	4.120	0.261
Dark	1.131	2.759	0.410	0.716	0.820	0.193	0.0001	5.137	64.014

**Table 4** – Solar cell parameters of the device ITO / PEDOT : PSS / P3HT : ZnS<sub>Hexa</sub> / Al

Mode	$P_{max}$ , nW	$I_{pm}$ , nA	$V_{pm}$ , V	$J_{sc}$ , $\mu\text{A}/\text{cm}^2$	$V_{oc}$ , V	$FF$	$E_{ff}$ , %	$r_s$ , M $\Omega$	$r_{sh}$ , M $\Omega$
Light	323.317	769.802	0.420	229.60	1.300	0.108	0.0320	1.765	0.124
Dark	8.293	17.277	0.480	3.74	0.959	0.231	0.0008	22.261	17.846

**Table 5** – Solar cell parameters of the device ITO / PEDOT : PSS / P3HT : ZnS<sub>Hexa</sub> : Ag-PVA / Al

Mode	$P_{max}$ , nW	$I_{pm}$ , nA	$V_{pm}$ , V	$J_{sc}$ , $\mu\text{A}/\text{cm}^2$	$V_{oc}$ , V	$FF$	$E_{ff}$ , $10^{-6}$ %	$r_s$ , M $\Omega$	$r_{sh}$ , M $\Omega$
Light	0.092	0.541	0.17	0.024	0.376	0.257	2.300	429	329
Dark	0.017	0.438	0.12	0.019	0.352	0.064	0.425	52	61

particles. Excitation of LSPR within metal nanoparticles can create strong near-field electromagnetic fields and far-field propagating waves that enhance the light absorption and photocurrent of organic photovoltaic devices [29, 30]. Recent studies have shown that hybrid organic photovoltaic devices with metal particles incorporated in the photo-active region have enhanced light absorption and photocurrent [31]. However, the power conversion efficiency (PCE) in these cases might be restricted by exciton quenching with non-radiative energy transfer and the differences between the electronic properties of the metal nanoparticles and the conjugated molecules in the hybrid material.

Sefunc et al. [17] present surface plasmon polariton assisted thin-film organic solar cells made of P3HT : PCBM based on plasmonic back contact grating architecture for enhancing optical absorption under TM- and TE-polarization within the most effective spectral range of AM1.5G solar radiation. They have analyzed two plasmonic structures embedded into the organic solar cell architecture comprised of glass / ITO / PEDOT : PSS / P3HT : PCBM / Ag [17] and the metal grating is made of Ag and found that the absorption of the active materials is increased upto 21 % [17]. Group of Fang Cheng et al. [32] embedded the Au metallic nano structures in the PEDOT : PSS buffer layer to improve the device performance of P3HT : PCBM devices.

Mie Xue et al. [26] reports a structure ITO / PEDOT : PSS / P3HT : PCBM : Ag nanoparticles / Al structure and showed that the efficiency decreased upon the addition of Ag nanoparticles but the carrier mobility in P3HT : PCBM bulk heterojunction device increases with increasing concentration of the Ag nanoparticles, since the metal particles act as carrier traps so that recombination occurs at the interface of metal nano particles and P3HT. The reported cell of P3HT : PCBM has shown an efficiency about 3.4 % but the addition of Ag nanoparticles at a 1 : 16 (Ag : P3HT) weight ratio lowered the device efficiency to 3.3 % [26]. Where each Ag nanoparticle acts as a hopping site and the average hopping distance becomes smaller as the

nanoparticle density in the active layer increases that increases mobility, but carriers are trapped on the nanoparticle traps that decreases the extracted charge carriers. Since the device power conversion efficiency is proportional to both the number of extracted carriers and their mobility, the substantial decrease in the number of extracted carriers subdue the smaller mobility increase, resulting in the net lower device efficiency.

In the previous studies the metal nanoparticles were in direct contact with the active layer, therefore the generated excitons can be quenched at the metal nano particles. In order to avoid this, coating over the metal nano particles is required. From our previous experiments [18], the optimized PVA coated silver nano particle sample was chosen for this experiment that the sample was selected since it has highest absorption.

$J$ - $V$  characteristics of the fabricated ITO / PEDOT : PSS / P3HT : ZnS<sub>Hexa</sub> : Ag-PVA / Al device is shown in figure 8 and the solar cell parameters are shown in Table 5. When comparing with the other two cells without the Ag nanomaterials,  $I_{sc}$ ,  $V_{oc}$  and efficiency decreased well but shunt resistance increased much thereby fill factor also. The reduction in the cell parameters may be due to the inhomogeneity of the polymer matrix due to the introduction of the non-conductive polymer PVA.  $I_{sc}$  decreased due to the reduction of mobility since the metal nano particles are not in direct contact with the conductive polymer P3HT. This results shows that the introduction of metal nano particles in to the active layer with or without coating of non-conductive polymers reduces the cell performance.

Table 6 compares the cell parameters of prepared solar cells with the previously reported P3HT : ZnS bulk heterojunction solar cells. It is very clear from the Table 6 that the cell made with ZnS<sub>Hexa</sub> has higher  $V_{oc}$  than the other reported ZnS<sub>CUBIC</sub> made solar cells. The maximum efficiency obtained in this work (0.032 %) is good as the previously reported P3HT : ZnS bulk heterojunction solar cell [11], but it is not higher than the best current devices current devices of P3HT : PCBM + TiO<sub>2</sub> nano tubes (4.07 %) [33],

**Table 6** – Comparison of cell parameters of the prepared cell with published P3HT : ZnS based cells

Sample	Particle size, nm	$V_{oc}$ , V	$J_{sc}$ , $\mu\text{A}/\text{cm}^2$	$FF$	Efficiency, %
P3HT:ZnS <sub>Cubic</sub> (1 : 0.1) [4]	4-6	0.64	10.60	0.27	0.0023
P3HT:ZnS <sub>Cubic</sub> (1 : 1) [13]	10	1.20	8.10	0.25	0.2
P3HT:ZnS <sub>Cubic</sub> (1 : 0.05)	1.46	1.2	30.100	0.109	0.0037
P3HT:ZnS <sub>Hexa</sub> (1 : 0.05)	3.2	1.3	229.60	0.108	0.032

P3HT: ICBA (6.5 %) [8] and PTB7: PC71BM (7.4 %) [34]. The improvement demonstrated in this work is therefore an improvement in the research on the devices made with the blend of P3HT / ZnS<sub>Cubic</sub>, P3HT / ZnS<sub>Hexa</sub> and P3HT : ZnS<sub>Hexa</sub> : PVA-Ag.

#### 4. CONCLUSION

It is shown that device of P3HT : ZnS can give higher  $V_{oc}$  and hexagonal ZnS can improve the cell parameters further. Surface modified wurtzite ZnS is able to give higher  $V_{oc}$  as well as higher current density and comparable efficiency. Even though, this device was not able to give higher efficiency when compared to the previously reported P3HT : PCBM based devices, since

the ZnS don't readily form a good charge separation interface with P3HT. The second reason may be the structural parameters that the nano absorbing materials are aggregated. It remains an open challenge to synthesize uniformly dispersed particles in P3HT polymer matrix to enable the fabrication of highly efficient polymer-inorganic solar cell due to the short exciton diffusion length of the popular polymer.

#### ACKNOWLEDGEMENT

We acknowledge the support given by Arun D. Rao and Dr. Praveen C. Ramamurthy (Department of materials engineering), INUP and CEN @ IISc., Bangalore for completing this work.

#### REFERENCES

1. *Polymer solar cells, Aalborg university, faculty of physics and nanotechnology, project group: n440b* (2006).
2. René Janssen, *Introduction to polymer solar cells, project :3y280, departments of chemical engineering & chemistry and applied physics, Eindhoven university of technology, the Netherlands.*
3. David Ian Black, *Fabrication Of Hybrid Inorganic And Organic Photovoltaic Cells, Phd Thesis* (Emerging Technologies Research Centre, De Montfort University: Leicester, London: 2011)
4. H.E. Unalan, P. Hiralal, D. Kuo, B. Parekh, G. Amaratunga, M. Chhowalla, *J. Mater. Chem.* **18**, 5909 (2008).
5. J.U. Lee, J.W. Jung, T. Emrick, T.P. Russell, W.H. Jo, *J. Mater. Chem.* **20**, 3287 (2010).
6. G. Zhao, Y. He, Y. Li, *Adv. Mater.* **22**, 4355 (2010).
7. B.R. Saunders, M.L. Turner, *Adv. Colloid Interf. Sci.* **138**, 1 (2008).
8. A. Kongkanand, K. Tvrđy, K. Takechi, M. Kuno, P.V. Kamat, *J. Am. Chem. Soc.* **130**, 4007 (2008).
9. W. Martienssen, H. Warlimont, *Springer Handbook Of Condensed Matter And Materials Data, Ed. 1*, (Springer: New York: 2005).
10. Y. Yang, S. Xue, S. Liu, J. Huang, J. Shen, *Appl. Phys. Lett.* **69**, 377 (1996).
11. M. Bredol, K. Matras, A. Szatkowski, J. Sanetra, A.P. Schwa, *Sol. Energ. Mater. Sol. C.* **93**, 662 (2009).
12. M. Mall, P. Kumar, S. Chand, L. Kumar, *Chem. Phys. Lett.* **495**, 236 (2010).
13. S. Mokkalapati, F. Beck, K. Catchpole, *Plasmonic Solar Cells: Status And Prospects, SPIE Newsroom* (2010).
14. C. Min, J. Li, G. Veronis, J. Lee, S. Fan, P. Peumans, *Appl. Phys. Lett.* **96**, 133302 (2010).
15. H. Shen, P. Bienstman, B. Maes, *J. Appl. Phys.* **106**, 073109 (2009).
16. F.J. Beck, S. Mokkalapati, A. Polman, K.R. Catchpole, *Appl. Phys. Lett.* **96**, 033113 (2010).
17. M.A. Sefunc, A.K. Okyay, H.V. Demir, *Opt. Express* **19**, 14200 (2011).
18. T. Abdul Kareem, A. Anu Kaliani, *Arabian J. Chem.* **4**, 325 (2011).
19. T. Sun, Z.L. Wang, Z.J. Shi, G.Z. Ran, W.J. Xu, Z.Y. Wang, Y.Z. Li, L. Dai, G.G. Qin, *Appl. Phys. Lett.* **96**, 133301 (2010).
20. J. Deboisblanc, *Synthesis And Characterization Of P3ht : Pcbm Organic Solar Cells, Senior Thesis*, (Department Of Physics And Astronomy, Pomona College: California: 2010).
21. K.N. Rao, *Indian J. Pure Appl. Phys.* **42**, 201 (2004).
22. E.J. Guo, H. Guo, H. Lu, K. Jin, M. He, G. Yang, *Appl. Phys. Lett.* **98**, 011905 (2011).
23. R.H. Friend, R.W. Gymer, A.B. Holmes, J.H. Burroughes, R.N. Marks, C. Taliani, D.D.C. Bradley, D.A.D. Santos, J.L. Bre  das, M. Lo  gdlund, W.R. Salaneck, *Nature* **397**, 121 (1999).
24. L.M. Chen, Z. Xu, Z. Honga, Y. Yang, *J. Mater. Chem.* **20**, 2575 (2010).
25. V.P. Devarajan, D. Nataraj, T. Pazhanivel, K. Senthil, M. Seol, K. Yong, J. Hermannsdorfer, R. Kempe, *J. Mater. Chem.* **22**, 18454 (2012).
26. Z. Hu, T. Daeri, M.S. Bonner, A.J. Gesquiere, *J. Lumin.* **130**, 771 (2010).
27. U. Zhokhavets, T. Erb, H. Hoppe, G. Gobsch, N.S. Sariciftci, *Thin Solid Films* **496**, 679 (2006).
28. J. Guo, H. Ohkita, H. Benten, S. Ito, *J. Am. Chem. Soc.* **132**, 6154 (2010).
29. I.K. Ding, J. Zhu, W. Cai, S.J. Moon, N. Cai, P. Wang, S.M. Zakeeruddin, M. Gr  tzel, M.L. Brongersma, Y. Cui, M.D. Mcgehee, *Adv. Energ. Mater.* **1**, 52 (2011).
30. J.H. Lee, J.H. Park, J.S. Kim, D.Y. Lee, K. Cho, *Organic Electron.* **10**, 416 (2009).
31. A.P. Kulkarni, K.M. Noone, K. Munchika, S.R. Guyer, D.S. Ginger, *Nano Lett.* **10**, 1501 (2010).
32. Y. Yang, W. Guo, Y. Zhang, Y. Ding, X. Wang, Z.L. Wang, *Nano Lett.* **11**, 4812 (2011).
33. G.K. Mor, K. Shankar, M. Paulose, O.K. Varghese, C.A. Grimes, *Appl. Phys. Lett.* **91**, 152111 (2007).
34. Y. Liang, Z. Xu, J. Xia, S.T. Tsai, Y. Wu, G. Li, C. Ray, L. Yu, *Adv. Mater.* **22**, E135 (2010).